Sensors and Materials, Vol. 38, No. 8 (2026) 4975–4990
MYU Tokyo

S & M 4605

Development of a Prussian-blue-based Cesium Adsorption and Real-time Monitoring System for Aqueous Environments

SuJung Min,[1] SuJin Kim,[2] BumKyoung Seo,[1] and SangBum Hong[1,2*]

[1]Department of Nuclear Facility Cleanup Technology, Korea Atomic Energy Research Institute (KAERI), 111 Daedeok-daero 989beon-gil, Yuseong-gu, Daejeon 34057, Republic of Korea
[2]Nuclear Science and Technology, University of Science and Technology (UST), 217 Gajeong-ro, Yuseong-gu, Daejeon 34113, Republic of Korea

(Received November 24, 2025; accepted August 17, 2026)

Keywords: Prussian blue, real-time monitoring, adsorption, Cs-137, removal rate

Radioactive cesium, particularly Cs-137, poses a long-term environmental and health risk owing to its long half-life and high solubility and mobility in aquatic environments. To enable efficient removal and real-time monitoring, in this study, we developed a closed-loop adsorption–detection system employing Prussian blue (PB) as a selective adsorbent. The system consists of two sequential adsorption modules housed in 1 L Marinelli beakers filled with PB-alginate beads. A NaI(Tl) detector (1st module) and a $LaBr_3$ detector (2nd module) were installed to enable continuous in situ gamma spectrometric monitoring. The adsorption performance of PB-alginate beads was initially evaluated using nonradioactive and radioactive Cs solutions. Nonradioactive tests using stable Cs solutions (5 and 50 ppm) demonstrated rapid adsorption, achieving removal efficiencies of 81 and 41% within 10 min, respectively. The distribution coefficient (K_d) analysis revealed a higher K_d at a low concentration (4.26 mL/g at 5 ppm) than at high concentration (0.695 mL/g at 50 ppm), suggesting that adsorption efficiency decreased under a high-concentration conditions because of the limited availability of adsorption sites. Radioactive Cs-137 tests validated the system's real-time monitoring capability, achieving an overall removal efficiency of approximately 90%. These results indicate that the PB-alginate bead-based closed-loop system enables effective Cs-137 adsorption and real-time quantification, offering a promising platform for radiological emergency response and environmental remediation. By integrating PB-alginate bead-based adsorption with NaI(Tl) and $LaBr_3$ detectors, the proposed system enables the continuous real-time monitoring of radioactive cesium in aqueous environments, demonstrating its applicability as a sensor-based monitoring system.

1. Introduction

Radioactive cesium is one of the major radionuclides generated from nuclear power generation, spent fuel reprocessing, and nuclear weapons testing. Owing to its high mobility and solubility, and long-term persistence in aquatic environments, continuous radiological

*Corresponding author: e-mail: sbhong@kaeri.re.kr
https://doi.org/10.18494/SAM6205

ISSN 0914-4935

monitoring is essential for the early detection and management of radioactive contamination. However, the real-time monitoring of radioactive cesium in aqueous environments remains technically challenging because low radionuclide concentrations require high detection sensitivity while continuous measurements must be performed under dynamic flow conditions. Furthermore, conventional monitoring systems only detect radioactive contamination and do not provide the capability to remove radioactive cesium from contaminated water.[1–5] Therefore, there is a growing need for integrated technologies that combine selective adsorption materials with radiation detectors, enabling simultaneous radioactive cesium removal and real-time monitoring.

Since the Fukushima accident, the demand for the continuous in situ monitoring of low-concentration radioactive cesium over prolonged periods has increased, leading to the advancement of real-time underwater gamma spectrometry systems into in situ spectrometers and flow-through Marinelli-based online monitors. In 2021, Tsinghua University demonstrated the use of a $LaBr_3$(Ce) detector mounted on a buoy for in situ measurements, collecting and transmitting spectra at 5 min intervals over a long period. Dou *et al.* verified the energy resolution (2.6% at 662 keV) and field stability of the system through on-site demonstrations at the discharge outlet of a nuclear power plant in the southeastern coastal region of China.[6] In 2023, the Institute of Oceanography in Greece analyzed the activity concentration of naturally enriched radioactivity in natural drinking water contained in a large tank using the NaI(Tl)-based underwater gamma spectrometer KATERINA and the full spectrum analysis (FSA) method. By combining experimental data with data reproduced through MCNP simulations, a new calibration method was validated, enabling rapid quantitative measurements up to an energy of 2614 keV and demonstrating precise detection capabilities even in the high-energy region.[7] In 2024, Nanjing University in China reported that a shipborne system equipped with large NaI(Tl) detector arrays for mobile and wide-area monitoring reconstructed spatial distribution maps by combining in situ measurements taken during navigation with simulation data.[8] In 2023, the Institute of Oceanographic Instrumentation in China proposed an algorithmic methodology for automatic quantification and noise reduction based on the restoration of the response function of seawater gamma spectra, which improved spectrum reconstruction and peak separation performance.[9] In the field of real-time flow-through monitoring, NUVIATech's SAFEWATER Drinking Water Monitoring System has introduced commercial devices in which samples are filled into Marinelli beakers and surrounded by detectors [typically NaI(Tl) or $LaBr_3$], thereby reducing the minimum detectable activity (MDA). These systems support continuous measurements and remote alarm functions.[10] In this way, recent developments in marine monitoring systems have advanced through parallel research efforts, including the demonstration of in situ systems using various inorganic scintillation detectors, self-calibration techniques, wide-area real-time monitoring using shipborne platforms, low-MDA flow-through Marinelli-based devices, the establishment of open databases, and the advancement of analytical algorithms. These efforts are laying the technological foundation for the rapid, quantitative, and continuous monitoring of Cs-137.

Prussian blue (PB) has been widely studied and utilized as a representative adsorbent for the removal of cesium. PB has a three-dimensional lattice structure that contains cavities capable of

accommodating alkali metal ions, as well as vacancies generated during the synthesis process. The cesium adsorption behavior of PB is mainly explained by three mechanisms. First, there is an ion-exchange mechanism in which K^+, Na^+, and NH_4^+ ions within the PB lattice are exchanged with Cs^+, leading to the entrapment of cesium inside the structure. Because the ionic radius of Cs^+ is similar to that of K^+, this exchange reaction occurs favorably from a thermodynamic perspective. Second, the cavity (vacancy) size of PB (~3.2 Å) closely matches the ionic radius of Cs^+ (3.29 Å), allowing Cs^+ to be incorporated more stably than Na^+ or Ca^{2+}. Third, vacancies generated during the synthesis process act as defect-based adsorption sites for Cs^+ insertion. A high number of defects leads to a significant increase in adsorption capacity, making it a critical factor in determining the actual adsorption performance. It has been reported that the penetration of Cs^+ into the interior of PB crystals is limited, and that most of the adsorption occurs at a small depth of approximately 1–2 nm from the surface.[11] In addition, there are studies that have shown rapid cesium adsorption and high adsorption performance in defect-rich structures. In these cases, it has been reported that defect-rich structures play a significant role in enhancing adsorption performance, and that structural changes such as "wrinkles" can increase the effective surface area, thereby potentially improving both the adsorption rate and capacity.[12] Moreover, there are studies that have experimentally demonstrated that defect control in PB plays an important role in enhancing adsorption performance, as the presence of defects induces structural distortions within the particles, leading to improvements in both adsorption rate and capacity.[13]

Previous studies on real-time radiological monitoring have primarily focused on the detection and quantification of radioactive contaminants using in situ or flow-through monitoring systems. Although these systems enable continuous measurements without sample collection, they are limited to monitoring functions and cannot remove radioactive cesium from contaminated water. Consequently, when radioactive contamination is detected, additional treatment processes are required to remove the contaminants, making monitoring and remediation separate processes. Conversely, previous studies on PB-based adsorbents have mainly focused on improving cesium adsorption performance through material optimization. In most cases, adsorption performance has been evaluated by periodically collecting water samples followed by laboratory-based analyses. As a result, these approaches cannot continuously monitor changes in radioactivity during the adsorption process, making it difficult to immediately evaluate adsorption performance under operating conditions. Integrating selective adsorption with real-time radiological monitoring can overcome these limitations by simultaneously removing radioactive cesium while continuously monitoring changes in radioactivity. This integrated approach enables the continuous evaluation of adsorption performance during operation without additional sample collection or laboratory analysis and allows both contamination monitoring and decontamination to be performed within a single system. Such integration provides a more efficient strategy for the management of radioactive contamination in aqueous environments. On the basis of this concept, we developed a closed-loop adsorption–detection system by integrating PB-alginate beads with NaI(Tl) and $LaBr_3$ detectors in a 1 L Marinelli beaker, enabling simultaneous cesium removal and continuous real-time monitoring.

2. Methods

In this section, we describe the PB-alginate bead synthesis method and the measurement test conditions required to evaluate the performance and field applicability of the monitoring system utilizing PB-alginate beads.

The nonradioactive test was designed to evaluate the intrinsic adsorption capacity and affinity of the PB-alginate beads under controlled, off-line conditions using stable cesium and ICP-MS analysis, whereas the radioactive test was designed to demonstrate the real-time monitoring and combined removal–detection performance of the complete closed-loop system under realistic radioactive conditions using Cs-137 and gamma spectrometry.

2.1 Fabrication of PB-alginate beads

PB was prepared to perform adsorption experiments using the adsorbent. Figure 1 shows the PB preparation process. In this study, alginic acid sodium salt from brown algae (Sigma Aldrich, St. Louis, MO, USA), iron (III) ferrocyanide (Sigma Aldrich, St. Louis, MO, USA), and calcium chloride, granular (SHOWA, Akasaka, Tokyo, Japan) were used. To prepare a 4% sodium alginate solution and a 2.5% calcium chloride solution, 16 g of sodium alginate and 10 g of calcium chloride were added to 400 mL of distilled water, respectively, and mixed with a magnetic stirrer at 250 rpm for 24 h. For the synthesis of 2.5% PB–alginate beads, 10 g of iron ferrocyanide was added to the sodium alginate solution. The iron ferrocyanide mixed solution was then added dropwise into the 2.5% calcium chloride solution using a 20 mL syringe

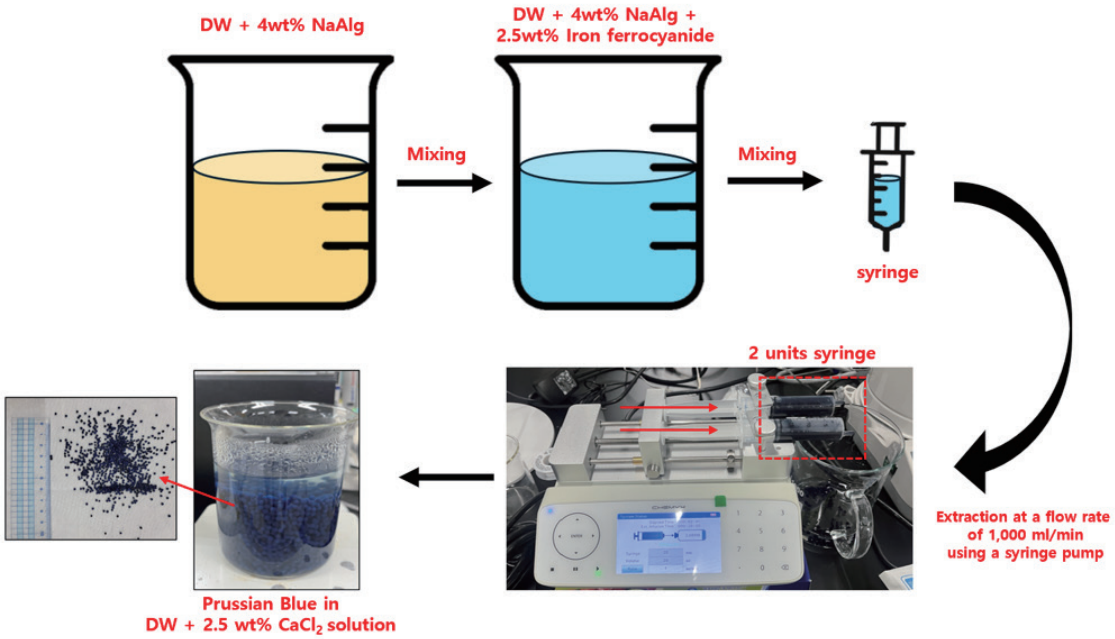

Fig. 1. (Color online) Prussian blue preparation process.

(KOVAX-SYRINGE) and a syringe pump (HARVARD APPARATUS 11 Plus). The syringe pump speed was set to 1000 mL/min to control the bead formation, resulting in spherical beads with an average diameter of approximately 3 mm.

2.2 MCNP simulation

Monte Carlo N-Particle (MCNP) simulation was performed to calculate the full-energy peak efficiencies of the NaI(Tl) and $LaBr_3$ detectors. In the simulation, the geometry and spatial arrangement of the 1 L Marinelli beaker and detectors were modeled to reproduce the actual experimental configuration, as shown in Fig. 2. The PB-alginate beads were assumed to be uniformly distributed inside the Marinelli beaker, and the Cs-137 source was homogeneously dispersed within a mixture of PB-alginate beads and water. To accurately represent the mixed medium, the bulk density of the PB-alginate bead–water mixture was calculated and applied as input to the MCNP model. The detector geometry was constructed on the basis of the actual dimensions, crystal materials, and shielding structure of the 3-inch NaI(Tl) and 2-inch $LaBr_3$ detectors. The gamma-ray energy of 662 keV, characteristic of Cs-137, was used in the simulation. The simulation was configured to record the photon flux incident on the active volume of the detectors and to tally the full-energy peak counts, which enabled the calculation of the detection efficiency. The calculated efficiencies were subsequently applied to convert the real-time spectral data into radioactivity values during the adsorption experiments.

2.3 Nonradioactive test

The nonradioactive experiment was conducted to evaluate the adsorption performance of the PB-alginate beads. The adsorption performance of the PB-alginate beads was evaluated using the removal efficiency and distribution coefficient (K_d). Cesium concentrations were determined by inductively coupled plasma–mass spectrometry (ICP–MS), and the adsorption performance

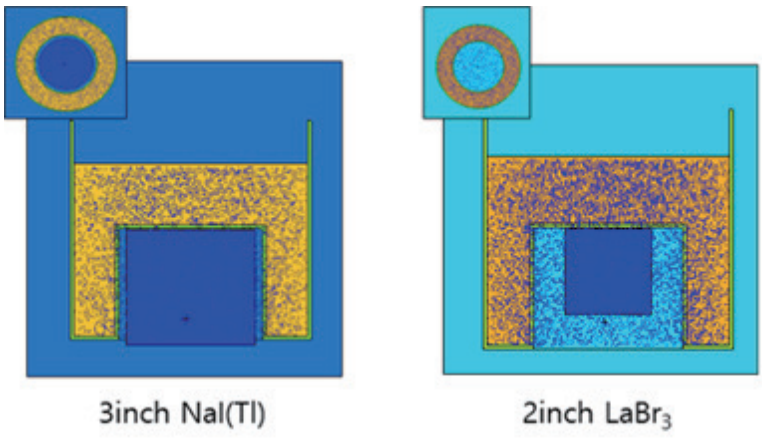

Fig. 2. (Color online) MCNP geometry for efficiency calculation of $LaBr_3$ and NaI(Tl) detectors.

was evaluated under both immersion and closed-loop circulation conditions. Adsorption performance tests were conducted using a cesium standard solution (Kanto Chemical Co., Inc., Tokyo, Japan) containing stable isotopes. The nonradioactive tests were carried out using two different methods: an immersion experiment and a closed-loop-type experiment. Figure 3 shows the immersion experiment, and Fig. 4 shows the closed-loop-type experiment. In the immersion experiment, Cs solutions diluted to concentrations of 5 and 50 ppm were used. The Cs solution and PB-alginate beads were mixed at a 1:1 ratio in a 50 mL conical centrifuge tube (standing type), and adsorption performance was evaluated after immersion for 0, 1, 3, 5, 7, 10, and 15 min.

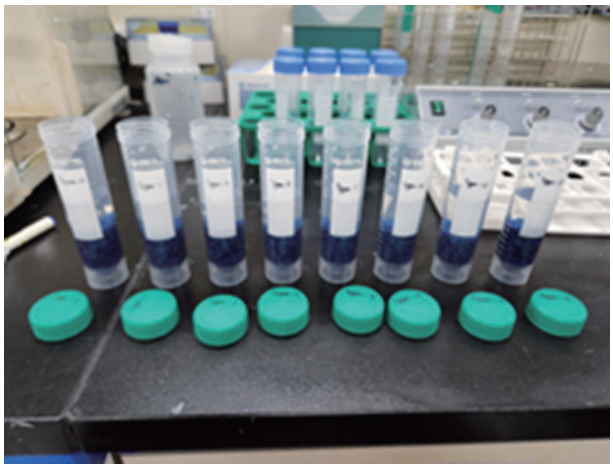

Fig. 3. (Color online) Immersion experiment using Cs standard solution.

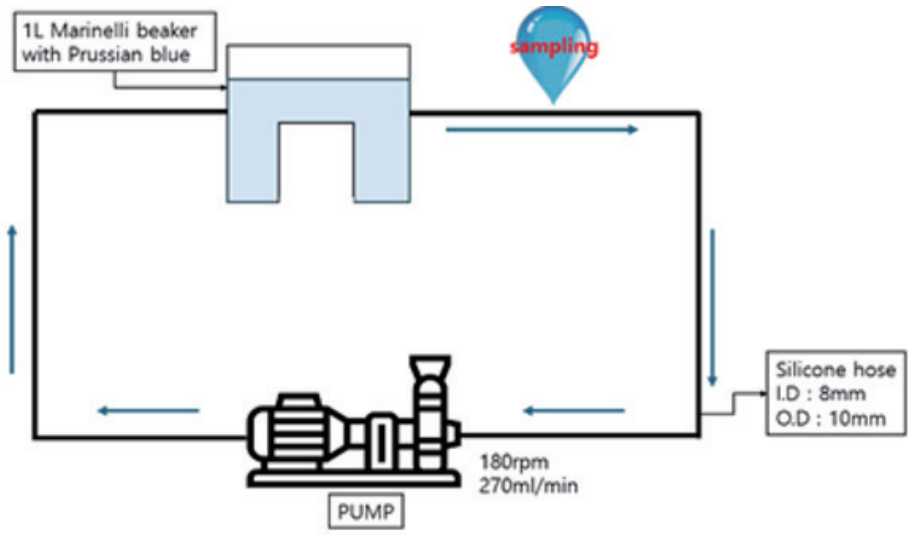

Fig. 4. (Color online) Closed-loop experiment using Cs standard solution.

The closed-loop-type experiment was conducted using standard cesium solutions diluted to concentrations of 5 and 50 ppm. A total of 125 g of PB-alginate beads and 250 mL of either the 5 or 50 ppm Cs solution were added to a 1 L Marinelli beaker. For the 5 ppm solution, 10 mL samples were collected using a syringe at predetermined sampling points after 0, 1, 3, 5, 7, 10, and 15 min. For the 50 ppm solution, considering the higher concentration, longer sampling intervals of 0, 10, 30, 60, 180, and 300 min were set, and 10 mL samples were collected in the same way. The flow rate was controlled at 270 mL/min (180 rpm) using a pump. Only one 1 L Marinelli beaker was used for the closed-loop-type experiment, and the sampling position is shown in the figure. The collected samples were analyzed by ICP–MS.

2.4 Radioactive test

The radioactive experiment was conducted using a Cs-137 solution to verify the real-time monitoring performance of the developed closed-loop adsorption system. NaI(Tl) and $LaBr_3$ detectors were used to continuously quantify the activity of Cs-137 adsorbed onto the PB-alginate beads during the adsorption process. For the radioactive test, a 3-inch NaI(Tl) detector and a 2-inch $LaBr_3$ detector were installed on separate 1 L Marinelli beakers to enable real-time measurements. Unlike the nonradioactive test, the radioactive test utilized two Marinelli beakers, and the system was designed so that residual nuclides not adsorbed in the first adsorption module can be captured in the second adsorption module, thereby improving the overall decontamination efficiency. A total of 500 g of PB-alginate beads was placed into each Marinelli beaker. To prevent the PB-alginate beads from obstructing the water flow or accumulating on one side due to the flow, the beads were placed inside a mesh and evenly distributed within the Marinelli beaker. Considering the volume of the two 1 L Marinelli beakers and the connecting hoses, the total volume of the circulating solution in the loop was calculated to be 2.1 L. A Cs-137 source was prepared by diluting the stock solution with distilled water to achieve a target activity concentration of 100 Bq/g. Spectra from both the first and second adsorption modules were acquired every 1 s, and the data were accumulated during the measurement. The pump flow rate was set to 270 mL/min (180 rpm), the same as in the nonradioactive test. The operating scheme of the radioactive test is shown in Fig. 5.

2.5 Calculation of adsorption performance

The cesium concentration was measured by ICP–MS, and the removal rate (R) was calculated as

$$R(\%) = \frac{C_0 - C_t}{C_0} \times 100, \tag{1}$$

where C_0 is the initial cesium concentration and C_t is the concentration at time t.

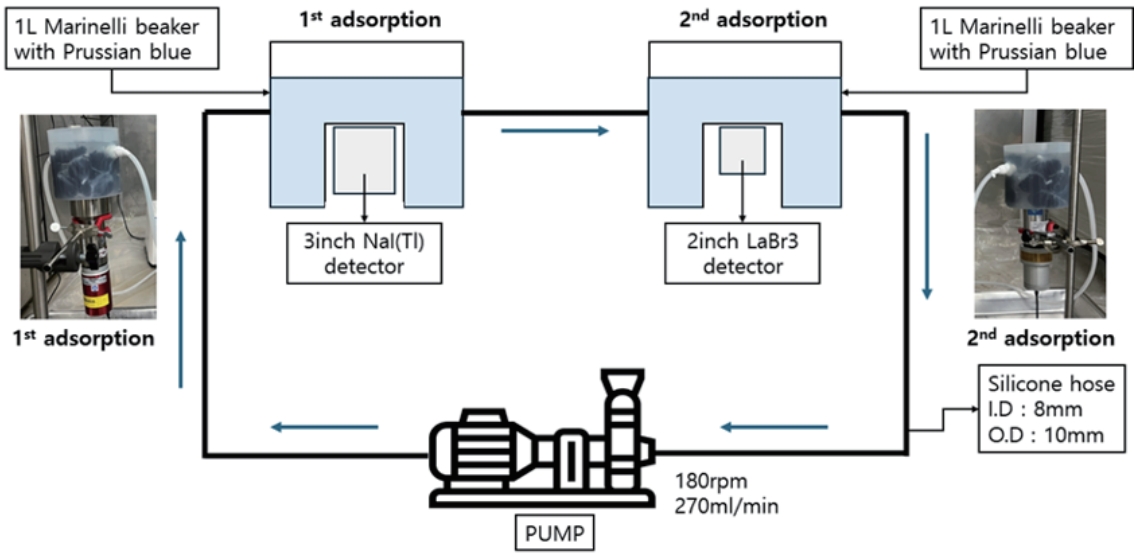

Fig. 5. (Color online) Closed-loop experiment using radioactive cesium.

The distribution coefficient (K_d) was calculated as

$$K_d\left(\mathrm{mL/g}\right)=\frac{\left(C_0-C_e\right)\times V}{C_e\times m}, \tag{2}$$

where C_e is the equilibrium concentration, V is the solution volume, and m is the mass of the adsorbent. The equilibrium concentration was obtained from the measured removal rate using

$$C_e=C_0\times\left(1-\frac{R}{100}\right). \tag{3}$$

For comparison between experimental conditions in this study, the ratio of solution volume to adsorbent mass (V/m) was kept constant. Therefore, the distribution coefficient can be expressed as

$$K_d\propto\frac{C_0-C_e}{C_e}=\frac{R}{100-R}. \tag{4}$$

2.6 Activity and removal efficiency calculation

The activity (A) was calculated from the real-time measured peak counts using the following equation:

$$A(t)=\frac{N_p(t)-B_p}{\varepsilon(E)\times P_\gamma(E)\times t}, \tag{5}$$

where $N_p(t)$ is the peak count at time t, B_p is the background count, $\varepsilon(E)$ is the detector efficiency, $P_\gamma(E)$ is the gamma emission probability, and t is the measurement time. In the radioactive test, the activity measured by the NaI(Tl) and $LaBr_3$ detectors represents the Cs-137 activity accumulated on the PB-alginate beads inside each Marinelli beaker, rather than the residual activity remaining in the circulating water. Therefore, the removal efficiency was calculated by comparing the accumulated activity adsorbed in each module with the initial total activity of Cs-137 introduced into the closed-loop system.

The removal efficiency of each adsorption module was calculated as

$$R_i(t) = \frac{A_i(t)}{A_0} \times 100, \tag{6}$$

where $R_i(t)$ is the removal efficiency of the i-th adsorption module at time t, $A_i(t)$ is the activity of Cs-137 accumulated on the PB-alginate beads in the i-th module, and A_0 is the initial total activity of Cs-137 introduced into the 2.1 L closed-loop system.

The total removal efficiency of the two-stage adsorption system was calculated by summing the activities measured in the first and second adsorption modules as

$$R_{total}(t) = \frac{A_1(t) + A_2(t)}{A_0} \times 100, \tag{7}$$

where $A_1(t)$ and $A_2(t)$ are the accumulated Cs-137 activities measured in the first and second adsorption modules, respectively. This calculation assumes that the activity accumulated on the PB-alginate beads represents the removed fraction of Cs-137 from the circulating solution within the closed-loop system.

3. Results

3.1 Properties of PB

The PB-alginate beads fabricated in this study had a diameter of approximately 3 mm, and the weight of a single PB-alginate bead was measured to be approximately 0.0275 g. In addition, when the surface of the PB-alginate beads was observed under an optical microscope, wrinkles such as those shown in Fig. 6 were observed. These wrinkles were formed owing to moisture evaporation, and they have the advantage of increasing the surface area, thereby improving the adsorption performance. The formation of surface irregularities or wrinkles can increase the surface area compared with a simple flat structure, and the wrinkled regions may exhibit partial lattice distortions or a higher density of defects, which can serve as additional active sites for adsorption.

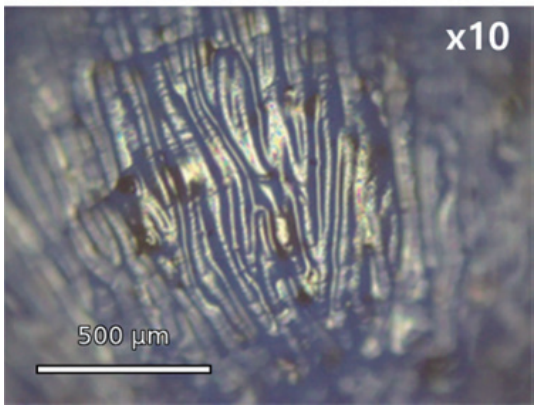

Fig. 6. (Color online) Prussian blue surface observed with an optical microscope (×10).

3.2 Results of nonradioactive test

Figure 7 shows the results of the immersion test. For the 5 ppm Cs solution (square points in Fig. 7), approximately 75% was adsorbed within 10 min. In contrast, for the 50 ppm solution (circle points in Fig. 7), about 40% was adsorbed after 10 min, and even after more than 300 min, the maximum adsorption reached only about 60%.

Figure 8 shows the results of the closed-loop test, which exhibited similar trends to the immersion test. For the 5 ppm Cs solution [Fig. 8(a)], approximately 81% was adsorbed within 10 min, whereas for the 50 ppm solution [Fig. 8(b)], about 40% was adsorbed after 10 min, and even after more than 300 min, the maximum adsorption reached only about 46%. The difference in adsorption performance between the 5 and 50 ppm solutions can be explained using the distribution coefficient (K_d) described in Sect. 2. The calculated C_e values were 0.95 ppm for the 5 ppm solution and 29.5 ppm for the 50 ppm solution. Accordingly, the calculated K_d values were 4.26 and 0.695 mL/g, respectively, indicating that the K_d value at 5 ppm was approximately 6.1 times higher than that at 50 ppm. The higher K_d value at the lower cesium concentration indicates a stronger distribution of Cs^+ toward the PB-alginate beads than the aqueous phase. In contrast, the lower K_d value at the higher concentration suggests that adsorption efficiency decreased under high-concentration conditions because more cesium ions competed for a limited number of available adsorption sites.

Overall, these results indicate that the adsorption performance of the PB-alginate beads decreased with increasing cesium concentration. In this study, the adsorption performance was evaluated using the removal efficiency and distribution coefficient (K_d). Further investigations incorporating adsorption equilibrium, adsorption kinetics, and breakthrough curve analyses under long-term continuous operation and various flow conditions are required to provide a more comprehensive understanding of the adsorption behavior and operational limit of the developed system.

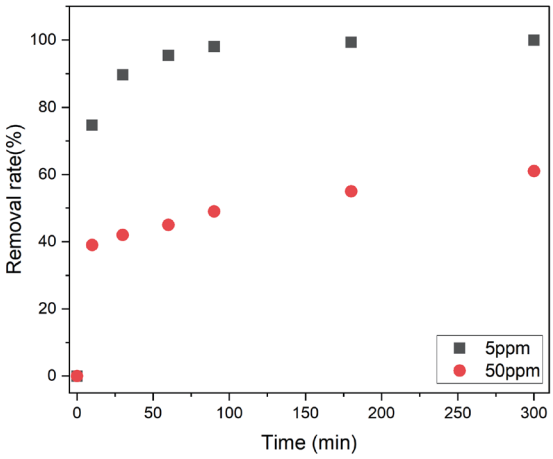

Fig. 7. (Color online) Immersion test results (square points: 5 ppm; circle points: 50 ppm).

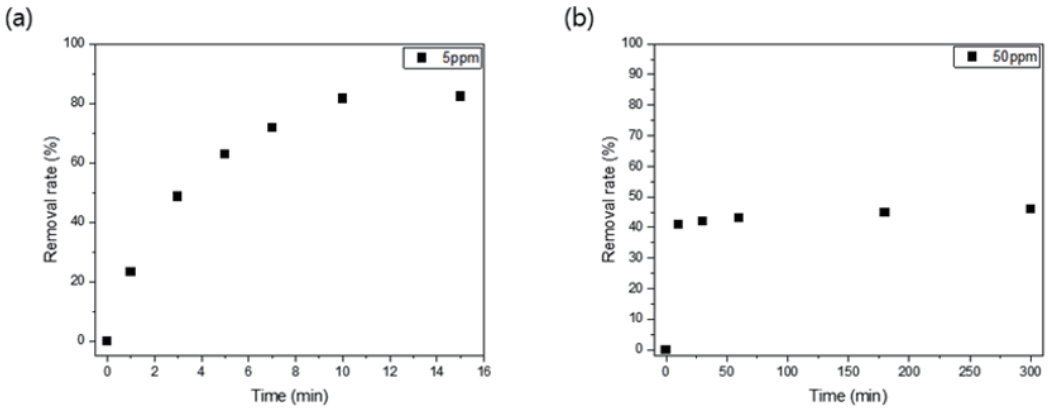

Fig. 8. (Color online) Closed-loop experiment results: (a) 5 ppm and (b) 50 ppm Cs solutions.

3.3 Results of radioactive test

In this study, a radioactive test was conducted using radioactive cesium to evaluate the performance of the real-time adsorption and monitoring system based on PB-alginate beads developed in this work. The removal rate during the radioactive test using radioactive isotopes was monitored in real time using $LaBr_3$ and NaI(Tl) detectors, and the data collected over 200 s were accumulated and analyzed. Figure 9 shows the variations in activity (Bq) and removal rate (%) as a function of time for the first adsorption module [measured by the NaI(Tl) detector] and the second adsorption module (measured by the $LaBr_3$ detector). The system was operated under a closed-loop condition with a constant flow rate, enabling the continuous real-time monitoring of Cs-137 adsorption during circulation.

In this experiment, the efficiency $\varepsilon(E)$ values for the NaI(Tl) and $LaBr_3$ detectors were obtained through MCNP simulation. The detectors and 1 L Marinelli beaker were modeled

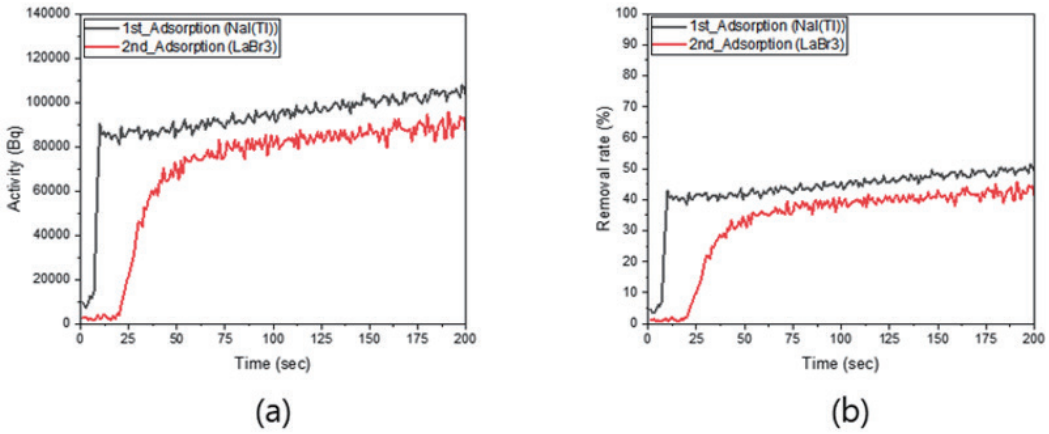

Fig. 9. (Color online) (a) Real-time radioactivity measurement and (b) removal efficiency in the first and second adsorption modules.

under the same geometric conditions, and simulations were performed at the Cs-137 gamma energy (662 keV) to calculate the peak efficiency. The simulation results showed that the peak efficiency of the NaI(Tl) detector was approximately 4% (@ 662 keV), whereas that of the $LaBr_3$ detector was approximately 1.4% (@ 662 keV). These efficiency values were applied to the real-time measured data to convert the counts to activity.

In the first adsorption process, the activity increased rapidly within the first 30 s after the start of the experiment and then continued to increase gradually up to 200 s [Fig. 9(a)]. The removal rate increased rapidly from the beginning of the experiment and reached approximately 45–50% at 200 s [Fig. 9(b)]. These results indicate that cesium removal in the PB-alginate bead adsorption layer occurs very rapidly in the initial stage, and most of the cesium is effectively removed in the first adsorption module within a short time. However, a portion of the cesium remained unabsorbed after passing through the first adsorption module.

In the second adsorption process, a similar removal behavior was observed. Overall, the removal rate was slightly lower than that in the first adsorption module. The activity increased gradually with time, and the removal rate reached 35–40% after 200 s. This indicates that the residual cesium not adsorbed in the first module was effectively adsorbed in the second module.

By combining the Cs-137 removal rates of the first and second adsorption modules, the overall performance of the system was evaluated. The total removal rate increased continuously over time, reaching approximately 90% after 200 s (Fig. 10). This demonstrates that the two-stage adsorption module system achieved a higher cesium removal efficiency than a single adsorption module. Furthermore, by simultaneously using NaI(Tl) and $LaBr_3$ detectors, the NaI(Tl) detector was able to sensitively measure the total activity variation during the initial high-concentration stage, and the $LaBr_3$ detector provided sharper resolution for low-activity detection, confirming quantitative accuracy during the later adsorption stages.

In this study, the detection efficiencies of the NaI(Tl) and $LaBr_3$ detectors were obtained by MCNP simulations that reflected the experimental geometry of the 1 L Marinelli beaker and detector configuration. The calculated efficiencies were then applied to convert the measured

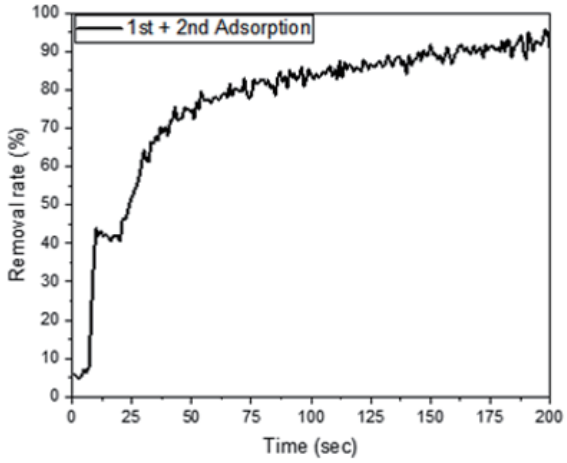

Fig. 10. (Color online) Total Cs-137 removal efficiency (%) of the first and second modules.

peak counts into Cs-137 activity. However, because the efficiencies were derived from simulations rather than experimental calibration with a standard radioactive source, several sources of uncertainty should be considered. These include possible differences between the modeled and actual detector dimensions, the crystal position, the dead layer or housing structure, the material composition, the density of the PB-alginate bead–water mixture, the source distribution inside the Marinelli beaker, and the relative position between the detector and the adsorbed Cs-137. In particular, the radioactive Cs-137 was progressively adsorbed onto the PB-alginate beads during circulation, whereas the MCNP model assumed a defined source distribution for efficiency calculation. Therefore, any deviation between the simulated source geometry and the actual time-dependent distribution of the adsorbed Cs-137 may affect the absolute activity values. For this reason, the activity and removal efficiency values obtained in this study should be interpreted considering the uncertainty associated with MCNP-derived efficiency. Nevertheless, the same MCNP-derived efficiencies were consistently applied to all time-dependent measurements for each detector, allowing the temporal changes in activity and the real-time monitoring behavior of the developed system to be evaluated under identical calculation conditions. Therefore, the present results are suitable for demonstrating the feasibility of real-time monitoring and comparing the relative adsorption behavior between the first and second adsorption modules. Future work will include experimental efficiency calibration using standard radioactive sources in the same Marinelli geometry to further validate the MCNP-based efficiency values and improve the accuracy of absolute activity quantification.

These radioactive test results show that the real-time adsorption and monitoring system developed in this study can achieve a high removal efficiency of radioactive cesium from aqueous solutions within a short period, while enabling activity calculation by applying MCNP-based efficiency values to real-time spectral data. This demonstrates the potential applicability of the system for actual contaminated water treatment and on-site real-time monitoring.

4. Conclusions

A novel closed-loop PB-based adsorption–detection system was developed for cesium removal and real-time monitoring using a 1 L Marinelli beaker packed with PB-alginate beads as an adsorbent, and its performance was quantitatively evaluated through nonradioactive tests (using stable isotopes) and radioactive tests (using radioactive isotopes). The system consisted of a two-stage adsorption module, comprising a first-stage NaI(Tl) module and a second-stage $LaBr_3$ module, with real-time gamma spectrometry conducted at each stage. For activity calculations, the detection efficiency was obtained and applied through MCNP simulations, reflecting the geometry of the 1 L Marinelli beaker. In the nonradioactive test, removal efficiencies of 81% within 10 min at 5 ppm and 41% at 50 ppm was observed. A comparison of the distribution coefficient (K_d) under the same conditions revealed that the K_d value at 5 ppm was approximately 6.1 times larger than that at 50 ppm, indicating excellent distribution and adsorption performance at low concentrations, suggesting reduced adsorption efficiency at high concentrations because of the limited availability of adsorption sites. In the radioactive test, the system achieved an overall removal efficiency of approximately 90% with continuous gamma monitoring enabled by dual detectors. This result clearly demonstrates the advantage of the two-stage adsorption configuration over a single-stage system.

The NaI(Tl) detector sensitively tracked the total activity variation during the initial high-concentration stage, whereas the $LaBr_3$ detector enabled high-resolution quantification of residual cesium in the low-concentration stage, highlighting their complementary roles.

In addition, optical microscopy observations revealed wrinkles and surface irregularities on the surface of the PB-alginate beads, which suggest the possibility of increased surface area and defect-related active sites. This contributes to enhanced initial adsorption rates and capacity, consistent with the initial rapid adsorption and subsequent gradual convergence behavior observed in both nonradioactive and radioactive tests.

Therefore, the developed system integrates (i) PB-alginate bead-based adsorption with NaI(Tl) and $LaBr_3$ detectors for simultaneous cesium removal and continuous real-time monitoring, (ii) the Marinelli geometry, which enables low-MDA detection even at low concentrations, (iii) real-time quantification based on MCNP-derived detection efficiency, and (iv) high-efficiency decontamination through two-stage adsorption modules. The developed system demonstrates the applicability of a sensor-based radiological monitoring platform for aqueous environments and provides a practical technological alternative for nuclear accident response, drinking water source protection, and continuous marine environmental monitoring. Future work will focus on the development of an open-loop monitoring system, automatic quantification, background correction during long-term continuous operation, on-site validation, and database integration. Such a system is expected to serve as a practical sensor-based platform that meets the requirements of rapid, quantitative, and continuous monitoring for both emergency response and routine environmental surveillance.

Acknowledgments

This work was supported by the Korea Atomic Energy Research Institute (KAERI) under Grant No. 522240-25.

References

1 Y. Ishii, S. S. Matsuzaki, and S. Hayashi: Data Brief **28** (2020) 105043. https://doi.org/10.1016/j.dib.2019.105043
2 Y. Ishii, S. S. Matsuzaki, and S. Hayashi: J. Environ. Radioact. **213** (2020) 106102. https://doi.org/10.1016/j.jenvrad.2019.106102
3 A. Abbasi: Mar. Pollut. Bull. **192** (2023) 114994. https://doi.org/10.1016/j.marpolbul.2023.114994
4 P. Saravanan, D. K. Anjan, S. Vharshini, B. Sowmya, E. A. Lopez-Maldonado, V. Saravanan, R. R. Kannan, M. Rajasimman, and S. Venkatkumar: Environ. Sci. Pollut. Res. **32** (2025) 15518. https://doi.org/10.1007/s11356-025-36651-6
5 J. W. Lee, S. D. Lee, H. B. Min, C. H. Han, and K. P. Kim: Appl. Radiat. Isot. **226** (2025) 112246. https://doi.org/10.1016/j.apradiso.2025.112246
6 D. Dou, Z. Zeng, W. Yu, M. Zeng, W. Men, F. Lin, H. Ma, J. Cheng, and J. Li: J. Mar. Sci. Eng. **9** (2021) 721. https://doi.org/10.3390/jmse9070721
7 C. Tsabaris, E. G. Androulakaki, and S. Alexakis: J. Mar. Sci. Eng. **11** (2023) 725. https://doi.org/10.3390/jmse11040725
8 Y. Shou, P. Gong, J. Zhang, Z. Wang, D. Liang, C. Zhou, and X. Tang: Nucl. Instrum. Methods Phys. Res. A **1069** (2024) 169946. https://doi.org/10.1016/j.nima.2024.169946
9 H. Bi, Y. Zhang, B. Wu, D. Yuan, X. Feng, and Y. Shi: Appl. Radiat. Isot. **198** (2023) 110853. https://doi.org/10.1016/j.apradiso.2023.110853
10 NUVIATech Instruments: NueM SafeWater. https://www.nuviatech-instruments.com/product/nuem-safewater (accessed August 2026)
11 H. Fujita, R. Miyajima, and A. Sakoda: Adsorption **21** (2015) 195. https://doi.org/10.1007/s10450-015-9662-z
12 Z. Wei, W. Zhao, J. Hu, T. Deng, and N. Zhang: Chem. Commun. **60** (2024) 396. https://doi.org/10.1039/D3CC05170F
13 J. H. Lee and S. Y. Kwak: ACS Omega **7** (2022) 3222. https://doi.org/10.1021/acsomega.1c05062

About the Authors

Su Jung Min received her Ph.D. degree from Kyung Hee University, Korea, in 2022. Since 2022, she has been working as a postdoctoral researcher at the Korea Atomic Energy Research Institute (KAERI). Her research interests include radiation measurement, sensor development, and the development of field radiation measurement technologies. (sjmin@kaeri.re.kr)

Su Jin Kim is currently studying for her master's degree at the University of Science and Technology (UST) and conducting research at the Korea Atomic Energy Research Institute (KAERI) in the areas of on-site radiation measurement and sensor development. (kimsujinn@kaeri.re.kr)

Bum Kyoung Seo received his Ph.D. degree from Pusan National University and is currently working as a researcher at the Korea Atomic Energy Research Institute (KAERI). He is an expert in decommissioning and decontamination technology development, as well as radiation measurement, and has contributed to nuclear site remediation and the enhancement of radiological environmental safety. (bumja@kaeri.re.kr)

Sang Bum Hong received his Ph.D. degree from Kyung Hee University and is currently working as a principal researcher at the Korea Atomic Energy Research Institute (KAERI). He is an expert in decommissioning and on-site radiation measurement, and has contributed to nuclear site remediation and the enhancement of radiological environmental safety. (sbhong@kaeri.re.kr)